Minimizing Reactive Current of a High Gain Dual Active Bridge Converter for Supercapacitor Based Energy Storage System Integration

Samir Hazra, Subhashish Bhattacharya
Electrical and Computer Engineering
North Carolina State University
Raleigh, USA
email: shazra, sbhatta4@ncsu.edu

***Abstract*—In this paper, a control strategy is presented to operate a dual active bridge (DAB) converter at optimal operating point in terms of minimized reactive component of current. To interface a supercapacitor based energy storage system with the dc grid to absorb oscillating energy a DAB can be used. A DAB can provide galvanic isolation and can cater high voltage gain required to integrate a low voltage supercapacitor module with a higher voltage dc-link (voltage ratio more than 5). During operation, the voltage of the supercapacitor varies in wide range due to storage of oscillating energy. Also, during charging of the supercapacitor from zero voltage at the start of the operation and discharging to zero voltage at the end of the operation the voltage ratio varies from ∞ to 1.0. Due to large deviation of the voltage ratio from unity the reactive power in the DAB is increased. To minimize the reactive power flow an optimization method based on fundamental components is presented in this paper. By reducing the reactive component of the current overall current of the DAB for a fixed power flow is reduced. Experimental results showing implementation of the optimal solution are presented.**

***Index Terms*—Energy storage system (ESS), Supercapacitor, Dual Active Bridge (DAB), Duty cycle modulation control, Phase-shift control.**

I. Introduction

Ocean wave energy can be harnessed to meet the growing demand of the energy consumption [1]. Majority of the WEC devices produce the oscillating power directly from the oscillating wave [2]–[4]. The generated power in the wave energy conversion system (WECS) oscillates at a frequency twice of the wave which has a dominant component of around $0.1\,\mathrm{Hz}$. Since, direct injection of the oscillatory power into the grid can cause voltage flickering and instability for the grid dynamics, smoothing of the WEC power is essential by integrating an energy storage device (ESD). Among various types of ESDs, batteries and supercapacitors can directly be integrated into the electrical circuit. The characteristics of the ESDs is attributed by its specific energy ($\mathrm{Wh/kg}$) and specific power ($\mathrm{kW/kg}$). The batteries have lower specific power due to the slow chemical reaction though it can store more energy per unit mass [5]. On the contrary, electrochemical devices like supercapacitors can be charged and discharged at a higher rate exhibiting higher specific power. However, supercapacitors can store relatively lower energy. Therefore, in systems with the requirement of absorbing short pulse of power the supercapacitor can be integrated. With the oscillating power the supercapacitor voltage fluctuates in a wide range [6].

Integration of supercapacitor based energy storage into dc bus can be done with different converters. Generally, the supercapacitor modules are built as low voltage high current energy storage devices. Therefore, to integrate the supercapacitor (48V) with the dc link (400 V) of the grid side converter, high voltage gain power converter is required. To achieve high voltage gain and high efficiency of the dc-dc power converter, a dual active bridge converter (DAB) is selected [7], [8]. With high gain DAB the major component of the converter loss is contributed from the conduction loss of the switches on the low voltage side. Therefore, in this work, the DAB is operated such that the conduction loss is minimized. The conduction loss can be minimized by minimizing the instantaneous reactive power in the converter. The reactive power is generated in DAB due to two reasons. Due to transformer leakage inductance a reactive power is associated with the active power at any operating condition which is influenced by the phase difference of the primary and secondary of the DAB. Also, due to the difference in voltage ratio and the turns ratio of the transformer, the reactive power is generated, increasing the current in the DAB.

In various studies it is attempted to minimize the rms current of the DAB [9]–[11]. However, the switching realization of the methods are complex. In this work a simple analytical solution is presented to compute the necessary duty cycle and phase difference, which is easy to implement. Through experiment the optimized duty cycle and phase shift are verified. Efficiency of the DAB operation is captured and presented.

II. Energy Storage for Wave Energy Conversion System

A typical system configuration of generating power in a wave energy conversion system is shown in Fig. 1. A generator connected to an oscillating wave energy converter (WEC) generates oscillating power [12]. To dispatch smooth power to the grid an energy storage system (ESS) can absorb the oscillating

978-1-4799-7312-5/18/$31.00 ©2018 IEEE

component of the generated power. A supercapacitor module can be appropriate to absorb oscillating power due to its higher specific power to energy ratio. Also, for better efficiency and higher voltage gain a dual active bridge converter can be preferred over a conventional dc-dc converter. Moreover, the transformer of the dual active bridge can provide the necessary galvanic isolation for the supercapacitor modules.

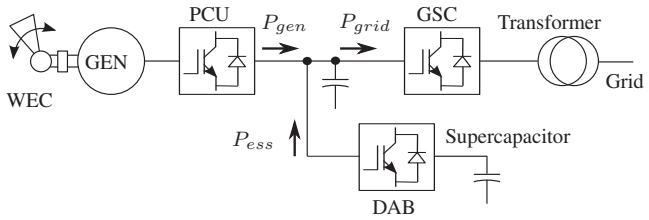

Fig. 1: Wave energy generation system with energy storage for smoothing oscillating power. Generator power conversion unit (PCU), grid side converter (GSC) and the dual active bridge (DAB) converter for integrating energy storage system are highlighted.

The primary focus of the paper is to minimize the reactive current in the DAB to enhance the efficiency. Due to oscillating power flow into the supercapacitor the terminal voltage of the supercapacitor modules also varies. However, the dc-link voltage of the system is regulated at a fixed value. As a result, the voltage gain of the DAB varies. Due to wide variation of the voltage gain reactive current flows in the DAB if the power in the DAB is controlled only by phase-shift between the primary and the secondary.

III. Fundamental Frequency Based Model of DAB

A DAB circuit diagram is shown in Fig. 2. For simplicity, in the analysis, the transformer turns ratio is assumed to be unity. The primary and secondary side dc bus voltages are considered to be v_{pdc} and v_{sdc} respectively. v_p and v_s are primary and secondary transformer voltages. i_p and i_s are primary and secondary transformer currents. The primary of the DAB is connected to the energy storage such as supercapacitor and the secondary side is connected to the dc link of the coupling of oscillating source like ocean wave generator and grid side power converter.

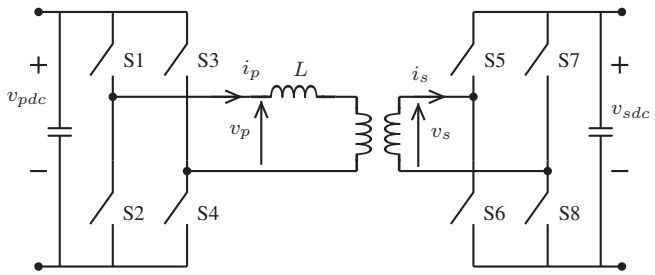

Fig. 2: Dual active bridge circuit. The secondary side of the circuit is referred to the primary to have transformer turns ration to be unity for analysis.

The primary and secondary voltage waveform is shown in Fig. 3. The phase angle lead of the primary voltage with respect to secondary is ϕ_{ps}. The duty ratio of primary and secondary voltage waveform is d_p and d_s respectively.

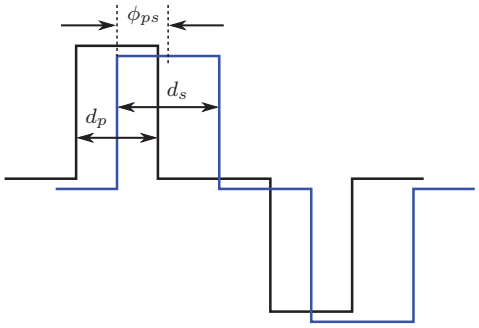

Fig. 3: DAB voltage waveform. ϕ_{ps} denotes the phase lead of the primary w.r.t. secondary voltage.

The square wave voltage outputs of the primary and secondary winding of the transformer are decomposed into its fundamental and harmonic components to analyze the power flow. The fundamental frequency of the voltage is the switching frequency. The leakage impedance of the transformer for n^{th} order harmonics of the switching frequency is, $X_n = 2\pi n f_{sw} L$. Where, f_{sw} and L are the switching frequency and leakage inductance of the transformer referred to primary.

Fourier analysis of the square wave voltage gives different frequency components of the transformer winding voltages as,

$$v_{pn} = \frac{4}{n\pi} \sin\left(\frac{n\pi}{2}\right) \sin\left(\frac{n\pi d_p}{2}\right) V_{pdc} \sin(2n\pi f_{sw} t) \quad (1)$$

$$v_{sn} = \frac{4}{n\pi} \sin\left(\frac{n\pi}{2}\right) \sin\left(\frac{n\pi d_s}{2}\right) V_{sdc} \sin(2n\pi f_{sw} t) \quad (2)$$

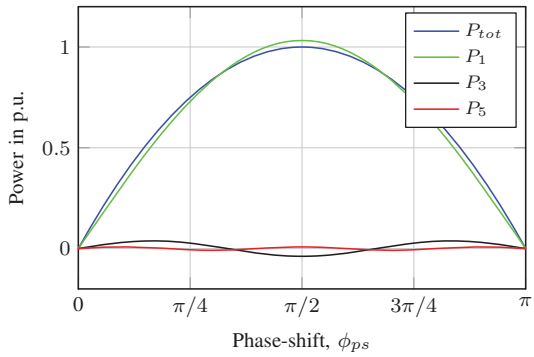

Fig. 4: Components of power. Contribution of harmonic components including third (P_3) and fifth (P_5) is negligible compared to fundamental component of the power (P_1).

The power flow in the DAB due to the fundamental and the harmonic components are plotted in Fig. 4. The power flow due to fundamental component, P_1 is close to the total power flow, P_{tot}. Since, the relative percentage of the higher order harmonics is negligible as shown in Fig. 4. In this analysis only fundamental power is considered. The fundamental voltage components are,

$$v_{p1} = \frac{4}{\pi} \sin\left(\frac{\pi d_p}{2}\right) V_{pdc} \sin(2\pi f_{sw} t) \quad (3)$$

$$v_{s1} = \frac{4}{\pi}\sin\left(\frac{\pi d_s}{2}\right) V_{sdc}\sin(2\pi f_{sw}t) \tag{4}$$

For the analysis the magnetizing component of the transformer considered to be small and negligible. The rms value of the fundamental voltage components (V_{p1} and V_{s1}) and primary current (I_{p1}) are,

$$V_{p1} = \frac{2\sqrt{2}}{\pi}\sin\left(\frac{\pi d_p}{2}\right) V_{pdc} \tag{5}$$

$$V_{s1} = \frac{2\sqrt{2}}{\pi}\sin\left(\frac{\pi d_s}{2}\right) V_{sdc} \tag{6}$$

$$I_{p1}^2 = \frac{1}{X_1^2}\left(V_{s1}^2 + V_{p1}^2 - 2V_{s1}V_{p1}\cos\phi_{ps}\right) \tag{7}$$

Considering ϕ_{ps} as the phase of the primary voltage with respect to secondary voltage, the fundamental component of the current is given as,

$$\begin{aligned} I_{p1}^2 = \frac{8}{\pi^2 X_1^2}\Bigg[&V_{sdc}^2\sin^2\left(\frac{\pi d_s}{2}\right) + V_{pdc}^2\sin^2\left(\frac{\pi d_p}{2}\right) \\ &- 2V_{sdc}V_{pdc}\sin\left(\frac{\pi d_s}{2}\right)\sin\left(\frac{\pi d_p}{2}\right)\cos\phi_{ps}\Bigg] \end{aligned} \tag{8}$$

The active power flow due to fundamental voltage is,

$$P_1 = \frac{8}{\pi^2 X_1}V_{sdc}V_{pdc}\left[\sin\left(\frac{\pi d_s}{2}\right)\sin\left(\frac{\pi d_p}{2}\right)\sin\phi_{ps}\right] \tag{9}$$

IV. Control Strategy

While interfacing energy storage devices such as supercapacitor, a DAB is controlled in power control mode. Whereas to bring the supercapacitor voltage to working range from its discharged state at the start of the energy storage operation current mode control is preferred. Similarly, to discharge the supercapacitor to zero voltage also the current mode control needs to be adopted.

In this particular application discussed in this paper, a supercapacitor with rated voltage of $48\,\mathrm{V}$ is interfaced with a dc bus of fixed voltage of $400\,\mathrm{V}$ to absorb the oscillating power. During charging of the supercapacitor, the supercapacitor voltage rises from zero to the operating value ($40\,\mathrm{V}$), while the voltage of the secondary side of the DAB is fixed at a rated voltage ($400\,\mathrm{V}$). Also, during the discharge of the supercapacitor the voltage is reduced from rated value to zero. Due to such wide variation of voltage gain between the primary and secondary (secondary to primary ratio varies from ∞ to 1.0) during charging and discharging of the supercapacitor, large reactive power flows through the DAB resulting increased loss. For fast charging and discharging, the DAB is expected to operate at the rated value of the rms current. Therefore, it is necessary that the charging and discharging occur at rated current while maximizing the active power transfer.

A. Maximization of Power with Constraint on rms Current by Lagrange Multiplier

With the limited current rating the charging of the supercapacitor can be accelerated if the power through the DAB is maximized by proper setting of phase difference (ϕ_{ps}) and duty cycle of the voltages (d_p, d_s). To maximize the power flow, only fundamental component of the DAB current is considered. Through optimization proper duty ratio and the phase difference of the voltages is evaluated. In the following optimization total power and current in the DAB are considered due to fundamental component only as given as,

$$I_p = I_{p1}, \quad P = P_1 \tag{10}$$

The problem definition: The power P needs to be optimized with constrained rms current of the DAB. In the total current the magnetizing component of the current is neglected.

From the expression of the fundamental current in (8) and the power in (9) the function to optimize is

$$P = \frac{8}{\pi^2 X_1}V_{sdc}V_{pdc}\sin\left(\frac{\pi d_s}{2}\right)\sin\left(\frac{\pi d_p}{2}\right)\sin\phi_{ps} \tag{11}$$

subject to the constrained function as given as,

$$\begin{aligned} \frac{I_p^2\pi^2 X_1^2}{8} &- V_{pdc}^2\sin^2\left(\frac{\pi d_p}{2}\right) - V_{sdc}^2\sin^2\left(\frac{\pi d_s}{2}\right) \\ &+ 2V_{sdc}V_{pdc}\sin\left(\frac{\pi d_s}{2}\right)\sin\left(\frac{\pi d_p}{2}\right)\cos\phi_{ps} = 0 \end{aligned} \tag{12}$$

With supercapacitor voltage less than the grid side dc link voltage, $V_{pdc} < V_{sdc}$, the duty ratio of the primary, d_p is set to maximum and the suitable ϕ_{ps} and d_s are found out through optimization. By defining the constants as,

$$\begin{aligned} k_0 &= -V_{sdc}^2 \\ k_1 &= \frac{I_p^2\pi^2 X_1^2}{8} - V_{pdc}^2\sin^2\left(\frac{\pi d_p}{2}\right) \\ k_2 &= -2V_{sdc}V_{pdc}\sin\left(\frac{\pi d_p}{2}\right) \\ k_p &= \frac{8}{\pi^2 X_1}V_{sdc}V_{pdc}\sin\left(\frac{\pi d_p}{2}\right) \end{aligned} \tag{13}$$

the optimization function can be written as,

$$f(d_s, \phi_{ps}) = k_p\sin\left(\frac{\pi d_s}{2}\right)\sin\phi_{ps} \tag{14}$$

The constraint function is given as,

$$\begin{aligned} g(d_s, \phi_{ps}) = k_1 + k_0\sin^2\left(\frac{\pi d_s}{2}\right) - k_2\sin\left(\frac{\pi d_s}{2}\right)\cos\phi_{ps} \\ = 0 \end{aligned} \tag{15}$$

The Lagrange function can be formed by combining the optimization function and the constraint function as,

$$\begin{aligned} L(d_s, \phi_{ps}, \lambda) &= f(d_s, \phi_{ps}) + \lambda g(d_s, \phi_{ps}) \\ &= k_p\sin\left(\frac{\pi d_s}{2}\right)\sin\phi_{ps} \\ &+ \lambda\left[k_1 + k_0\sin^2\left(\frac{\pi d_s}{2}\right) - k_2\sin\left(\frac{\pi d_s}{2}\right)\cos\phi_{ps}\right] \end{aligned} \tag{16}$$

where, λ is the Lagrange multiplier. By taking the partial derivative of the Lagrange function, $L(d_s, \phi_{ps}, \lambda)$ with respect to d_s, ϕ_{ps} and λ and setting to zero, it can be given as,

$$\frac{\partial L(d_s,\phi_{ps},\lambda)}{\partial d_s} = 0, \quad \Rightarrow k_p \cos\left(\frac{\pi d_s}{2}\right)\sin\phi_{ps} + \lambda\left[-k_2\cos\left(\frac{\pi d_s}{2}\right)\cos\phi_{ps} + k_0\sin\left(\pi d_s\right)\right] = 0 \quad (17)$$

$$\frac{\partial L(d_s,\phi_{ps},\lambda)}{\partial \phi_{ps}} = 0, \quad \Rightarrow k_p \sin\left(\frac{\pi d_s}{2}\right)\cos\phi_{ps} + \lambda\left[k_2\sin\left(\frac{\pi d_s}{2}\right)\sin\phi_{ps}\right] = 0 \quad (18)$$

$$\frac{\partial L(d_s,\phi_{ps},\lambda)}{\partial \lambda} = 0, \quad \Rightarrow k_1 + k_0\sin^2\left(\frac{\pi d_s}{2}\right) - k_2\sin\left(\frac{\pi d_s}{2}\right)\cos\phi_{ps} = 0 \quad (19)$$

Solving (18) it can be found that,

$$\sin\left(\frac{\pi d_s}{2}\right) = 0 \quad (20)$$

or

$$k_p\cos\phi_{ps} + \lambda k_2\sin\phi_{ps} = 0 \quad (21)$$

Replacing λ from (21) in (17) it gives,

$$k_p\cos\left(\frac{\pi d_s}{2}\right)\sin\phi_{ps} + \frac{-k_p\cos\phi_{ps}}{k_2\sin\phi_{ps}}\left[-k_2\cos\left(\frac{\pi d_s}{2}\right)\cos\phi_{ps} + k_0\sin\left(\pi d_s\right)\right] = 0$$

$$\Rightarrow k_p k_2\cos\left(\frac{\pi d_s}{2}\right)\sin^2\phi_{ps} + k_p k_2\cos\left(\frac{\pi d_s}{2}\right)\cos^2\phi_{ps} - k_p k_0\sin\left(\pi d_s\right)\cos\phi_{ps} = 0 \quad (22)$$

Since, $k_p \neq 0$, (22) simplifies to,

$$k_2\cos\left(\frac{\pi d_s}{2}\right) - 2k_0\sin\left(\frac{\pi d_s}{2}\right)\cos\left(\frac{\pi d_s}{2}\right)\cos\phi_{ps} = 0 \quad (23)$$

By solving (23) it can be given as,

$$\cos\left(\frac{\pi d_s}{2}\right) = 0, \quad \Rightarrow d_s = 1 \quad (24)$$

or

$$\cos\phi_{ps} = \frac{k_2}{2k_0\sin\left(\frac{\pi d_s}{2}\right)} \quad (25)$$

Since, $d_s = 1$ is the limiting solution, it is discarded. Combining (19) and (25) it becomes,

$$k_1 + k_0\sin^2\left(\frac{\pi d_s}{2}\right) - \frac{k_2^2}{2k_0} = 0 \quad (26)$$

By solving (26) the value of d_s can be found out as,

$$\sin\left(\frac{\pi d_s}{2}\right) = \sqrt{\frac{k_2^2 - 2k_0k_1}{2k_0^2}}$$

$$\Rightarrow d_s = \sin^{-1}\left(\sqrt{\frac{k_2^2 - 2k_0k_1}{2k_0^2}}\right)\frac{2}{\pi} \quad (27)$$

By inserting the solution of d_s in (25), the value of phase angle ϕ_{ps} can be given as,

$$\cos\phi_{ps} = \frac{k_2}{\sqrt{2(k_2^2 - 2k_0k_1)}} \quad (28)$$

In case of $V_{pdc} > V_{sdc}$, the primary duty ratio, d_p is varied and the constants needs to be modified as,

$$\begin{aligned} k_0 &= -V_{pdc}^2 \\ k_1 &= \frac{I_p^2\pi^2X_1^2}{8} - V_{sdc}^2\sin^2\left(\frac{\pi d_s}{2}\right) \\ k_2 &= -2V_{sdc}V_{pdc}\sin\left(\frac{\pi d_s}{2}\right) \\ k_p &= \frac{8}{\pi^2X_1}V_{sdc}V_{pdc}\sin\left(\frac{\pi d_s}{2}\right) \end{aligned} \quad (29)$$

The phase difference and duty cycle of the converters are given as,

$$\cos\phi_{ps} = \frac{k_2}{\sqrt{2(k_2^2 - 2k_0k_1)}} \quad (30)$$

$$d_p = \sin^{-1}\left(\sqrt{\frac{k_2^2 - 2k_0k_1}{2k_0^2}}\right)\frac{2}{\pi} \quad (31)$$

$$d_s = 1 \quad (32)$$

B. Minimization of RMS Current for Constraint Power Flow

In the operation of energy storage system, the voltage of the supercapacitor can have the ripple of around 20-30%. Therefore, the voltage ratio of the primary and secondary side dc link voltage deviates from the turns ratio of the transformer, which induces reactive current in the circuit. In this work, the rms current of the DAB is minimized to reduce the conduction loss in the DAB while transferring a particular amount of power. Therefore, the rms current is minimized with power as the constraint to find out appropriate phase difference, ϕ_{ps} and the duty ratio of the bridges d_p and d_s.

The problem definition: The rms current needs to be minimized with constrained power flow through the DAB. In the total current the magnetizing component of the current is neglected.

From the expression of fundamental current in (8) and the power in (9), the function to optimize is

$$\frac{I_p^2\pi^2X_1^2}{8} = V_{pdc}^2\sin^2\left(\frac{\pi d_p}{2}\right) + V_{sdc}^2\sin^2\left(\frac{\pi d_s}{2}\right) - 2V_{sdc}V_{pdc}\sin\left(\frac{\pi d_s}{2}\right)\sin\left(\frac{\pi d_p}{2}\right)\cos\phi_{ps} \quad (33)$$

subject to the constrained function as given as,

$$\frac{8}{\pi^2 X_1} V_{sdc} V_{pdc} \sin\left(\frac{\pi d_s}{2}\right) \sin\left(\frac{\pi d_p}{2}\right) \sin\phi_{ps} - P = 0 \quad (34)$$

With supercapacitor voltage less than the grid side dc link voltage, $V_{pdc} < V_{sdc}$, the duty ratio of the primary, d_p is set to maximum and the suitable ϕ_{ps} and d_s are found out through optimization. By defining the constants as,

$$\begin{aligned} k_0 &= -V_{sdc}^2 \\ k_3 &= V_{pdc}^2 \sin^2\left(\frac{\pi d_p}{2}\right) \\ k_2 &= -2V_{sdc}V_{pdc}\sin\left(\frac{\pi d_p}{2}\right) \\ k_p &= \frac{8}{\pi^2 X_1} V_{sdc} V_{pdc} \sin\left(\frac{\pi d_p}{2}\right) \end{aligned} \quad (35)$$

the optimization function can be written as,

$$f(d_s, \phi_{ps}) = k_3 - k_0 \sin^2\left(\frac{\pi d_s}{2}\right) + k_2 \sin\left(\frac{\pi d_s}{2}\right)\cos\phi_{ps} \quad (36)$$

The constraint function is given as,

$$g(d_s, \phi_{ps}) = k_p \sin\left(\frac{\pi d_s}{2}\right)\sin\phi_{ps} - P = 0 \quad (37)$$

The Lagrange function can be formed by combining the optimization function and the constraint function as,

$$\begin{aligned} L(d_s, \phi_{ps}, \lambda) &= f(d_s, \phi_{ps}) + \lambda g(d_s, \phi_{ps}) \\ &= k_3 - k_0 \sin^2\left(\frac{\pi d_s}{2}\right) + k_2 \sin\left(\frac{\pi d_s}{2}\right)\cos\phi_{ps} \\ &\quad + \lambda\left[k_p \sin\left(\frac{\pi d_s}{2}\right)\sin\phi_{ps} - P\right] \end{aligned} \quad (38)$$

By taking the partial derivative of the Lagrange function, $L(d_s, \phi_{ps}, \lambda)$ with respect to d_s, ϕ_{ps} and λ and setting to zero, it can be given as,

$$\begin{aligned} \frac{\partial L(d_s, \phi_{ps}, \lambda)}{\partial d_s} = 0, \quad &\Rightarrow -k_0 \sin(\pi d_s) + k_2 \cos\frac{\pi d_s}{2}\cos\phi_{ps} \\ &+ \lambda\left[k_p \cos\left(\frac{\pi d_s}{2}\right)\sin\phi_{ps}\right] = 0 \end{aligned} \quad (39)$$

$$\begin{aligned} \frac{\partial L(d_s, \phi_{ps}, \lambda)}{\partial \phi_{ps}} = 0, \quad &\Rightarrow -k_2 \sin\left(\frac{\pi d_s}{2}\right)\sin\phi_{ps} \\ &+ \lambda\left[k_p \sin\left(\frac{\pi d_s}{2}\right)\cos\phi_{ps}\right] = 0 \end{aligned} \quad (40)$$

$$\frac{\partial L(d_s, \phi_{ps}, \lambda)}{\partial \lambda} = 0, \quad \Rightarrow k_p \sin\left(\frac{\pi d_s}{2}\right)\sin\phi_{ps} - P = 0 \quad (41)$$

The solution from (40) can be given as,

$$\sin\left(\frac{\pi d_s}{2}\right) = 0 \quad (42)$$

or

$$-k_2 \sin\phi_{ps} + \lambda k_p \cos\phi_{ps} = 0, \quad \Rightarrow \lambda = \frac{k_2}{k_p}\tan\phi_{ps} \quad (43)$$

Substituting λ from (43), into (39) it is given as,

$$\begin{aligned} &-k_0 \sin(\pi d_s)\cos\phi_{ps} + k_2 \cos\frac{\pi d_s}{2}\cos^2\phi_{ps} \\ &\quad + k_2 \cos\left(\frac{\pi d_s}{2}\right)\sin^2\phi_{ps} = 0 \\ &\Rightarrow -k_0 \sin(\pi d_s)\cos\phi_{ps} + k_2 \cos\frac{\pi d_s}{2} = 0 \\ &\Rightarrow -2k_0 \sin\frac{\pi d_s}{2}\cos\frac{\pi d_s}{2}\cos\phi_{ps} + k_2 \cos\frac{\pi d_s}{2} = 0 \end{aligned} \quad (44)$$

The solutions of (44) are,

$$\cos\left(\frac{\pi d_s}{2}\right) = 0, \quad \Rightarrow d_s = 1 \quad (45)$$

or

$$\cos\phi_{ps} = \frac{k_2}{2k_0 \sin\frac{\pi d_s}{2}} \quad (46)$$

From (46) and (41), the phase difference, ϕ_{ps} can be computed as,

$$\phi_{ps} = \tan^{-1}\left(\frac{2k_0 P}{k_2 k_p}\right) \quad (47)$$

and subsequently, duty cycle, d_s can be computed as,

$$d_s = \sin^{-1}\left(\frac{P}{k_p \sin\phi_{ps}}\right)\frac{2}{\pi} \quad (48)$$

For the condition of $V_{pdc} > V_{sdc}$, only k_0 is modified as,

$$k_0 = -V_{pdc}^2 \quad (49)$$

V. Dual Active Bridge Design with high Voltage Gain

A. DAB Transformer Design

The DAB is designed to integrate the 48V supercapacitor module with the 400V dc link of the output side converter. The supercapacitor operating voltage is chosen to be 40V. The transformer is designed with a trans-ratio of 1:10. In the DAB, the primary side bridges are made with 100 V, 100 A Si MOSFETs. On the secondary side 600V Si IGBTs are used. The DAB is switched at 10 kHz. The leakage inductance of the transformer is 12.75 μH referred to low voltage side. The designed DAB converter is shown in Fig. 5.

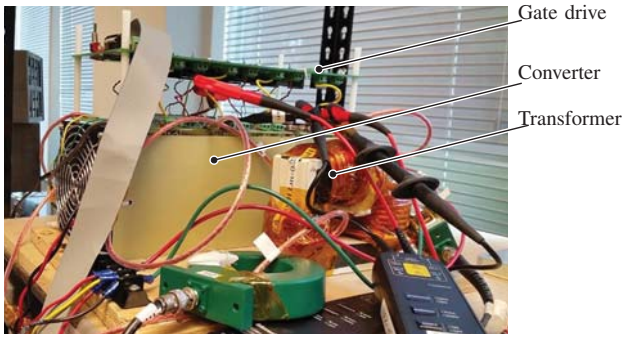

Fig. 5: DAB converter and transformer.

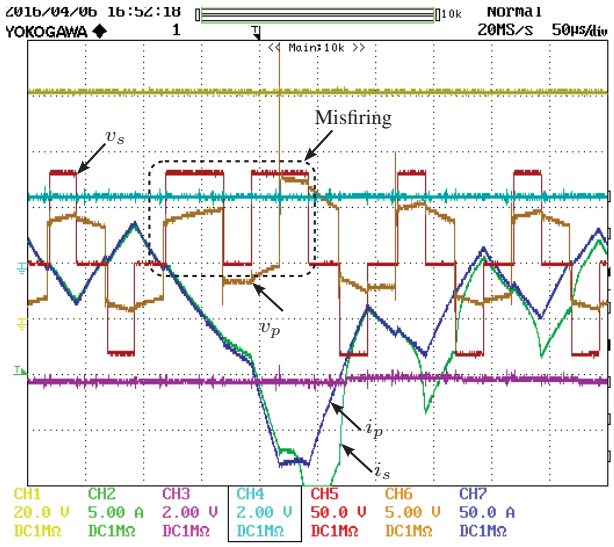

Fig. 6: Transformer saturation due to misfiring of the bridges.

B. DAB Switching Realization

To vary both duty ratio and phase of the bridges the switching of the DAB is carefully implemented. In this implementation DSP TMS320F28335 is used. The duty cycle update has a shadow register. However, any update of the phase is instantaneous. Therefore, during operation, when the corresponding counter values for both phase and duty ratio become same a compare event is skipped. Therefore, the switching of the DAB is also skipped for one leg, which results in volt-s buildup and saturates the transformer as shown in Fig. 6. To get rid of misfiring a distributed update technique is adopted.

C. Experimental Results

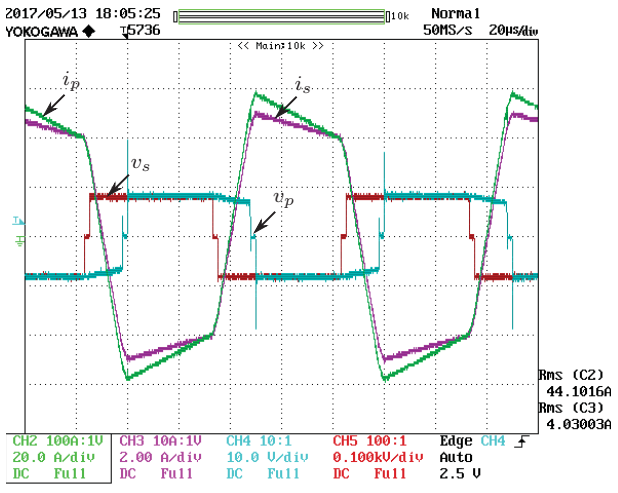

Fig. 7: DAB operation at supercapacitor charge mode at rms current of 40 A, 40V of supercapacitor voltage and 400 V of dc bus voltage. Scale: Ch5, v_s — 500 V/div, Ch3, i_s — 2 A/div, Ch4, v_p — 50 V/div, Ch2, i_p — 20 A/div.

Experimental results with a set value of rms current are presented. In Fig. 7 the rms current is set to 40 A on the primary side in charge mode of the supercapacitor. The operating voltage of supercapacitor and output dc link are 40 V and 400 V respectively. The duty cycle and phase angle between primary and secondary are computed from (27) and (28). The measured current on the primary and secondary side are 4.03 A and 44.1 A respectively. Since the voltage ratio is close to the turns ratio of the transformer the duty cycle of the primary and secondary voltages are close to unity. Current is generated by applying appropriate phase shift.

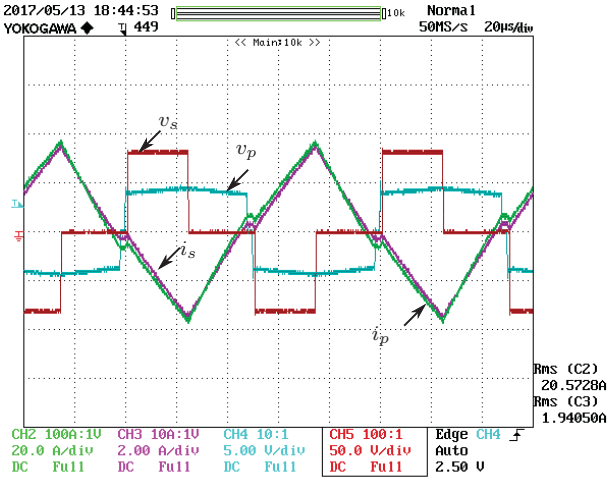

Fig. 8: DAB operation at supercapacitor charge mode at rms current of 20 A, 20V of supercapacitor voltage and 400 V of dc bus voltage. Scale: Ch5, v_s — 250 V/div, Ch3, i_s — 2 A/div, Ch4, v_p — 25 V/div, Ch2, i_p — 20 A/div.

In Fig. 8 the operating voltage of supercapacitor is 20 V while the output dc link voltage is fixed at 400 V. The rms current set point is 20 A. It can be seen that the duty cycle of the secondary voltage is reduced to minimize the reactive component of the current.

In Fig. 9, the waveforms for set rms current reference of 10 A respectively. It can be found that the rms current limit is closely followed to the set limit.

D. DAB Efficiency

The efficiency of the DAB is measured at different supercapacitor voltage, V_{pdc}. It can be seen that the efficiency of the converter is reduced at lower supercapacitor voltage. The maximum efficiency achieved at the nominal voltage of 40 V, is 95%. Due to the low efficiency of the DAB at lower supercapacitor voltage, the voltage ripple of the supercapacitor is kept limited to 20% of the nominal voltage.

E. Energy Storage Application

An emulated WEC system is developed to integrate the supercapacitor based energy storage system. As the system schematic described in 1 the generational system generates the oscillating power. The supercapacitor based energy storage system absorbs the oscillating component of the power and smoothed power is delivered to the grid.

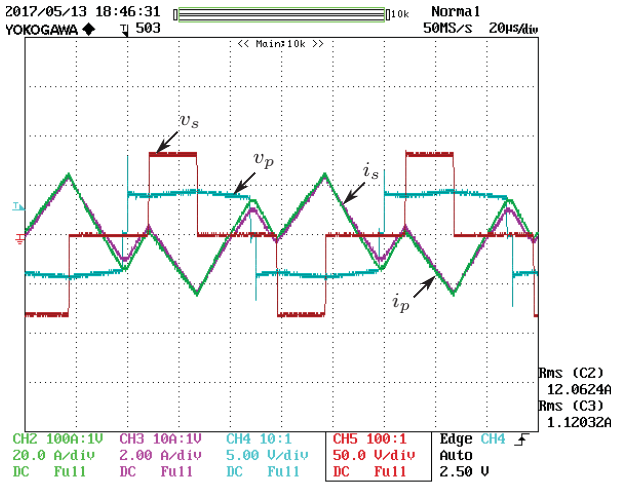

Fig. 9: DAB operation at supercapacitor charge mode at rms current of 10 A, 20V of supercapacitor voltage and 400 V of dc bus voltage. Scale: Ch5, v_s — 250 V/div, Ch3, i_s — 2 A/div, Ch4, v_p — 25 V/div, Ch2, i_p — 20 A/div.

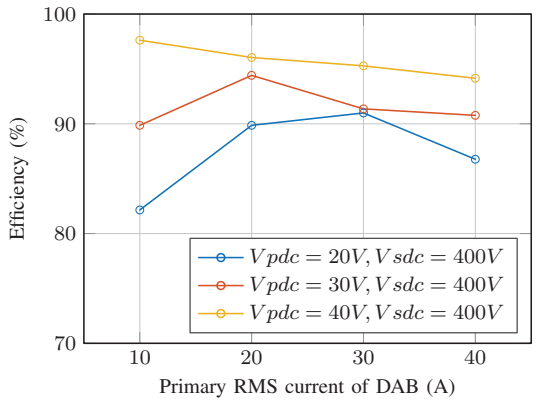

Fig. 10: Efficiency of the DAB at different supercapacitor voltage.

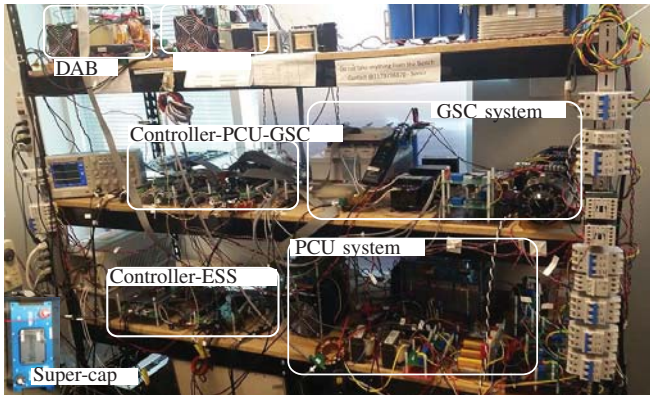

Fig. 11: Experimental test-bed for the grid tied wave energy and energy storage system implementation.

Control of the energy storage system (ESS) to absorb oscillating power from an wave energy conversion system (WECS) and to regulate the dc link voltage is demonstrated and result is shown in Fig. 12. In this test case, the generation of WECS is tied to the grid. Generated oscillating power P_{gen} and the controlled ESS power P_{ess} are shown in Fig. 12. Smoothed power P_{grid} from the WEC system is injected into the grid. The variation of the supercapacitor voltage is also captured from the experiment. V_{ess} is the voltage of the supercapacitor terminal.

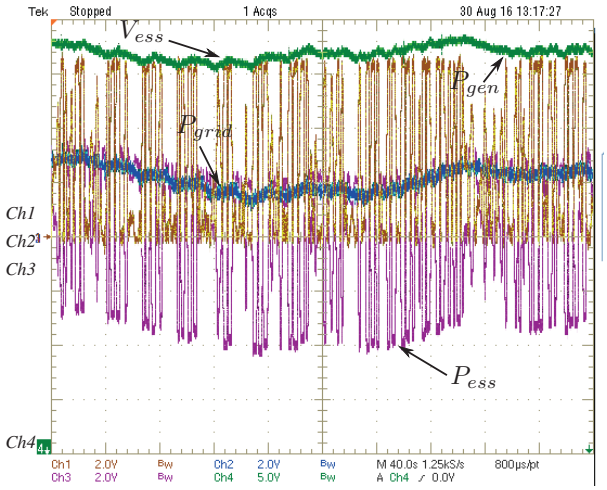

Fig. 12: WEC generation system connected to the grid with ESS regulating dc link voltage, Scale: Ch1, generated power, P_{gen}: 500 W/div, Ch2, smooth grid power, P_{grid}: 500 W/div, Ch3, power absorbed by ESS, P_{ess}: 500 W/div, Ch4, terminal voltage of ESS, v_{ess}: 5 V/div, time: 40s/div.

VI. Conclusion

In this work, the design and control of the DAB to maximize the efficiency is elaborated. The rms current of the DAB is minimized by minimizing the fundamental current of the DAB by properly controlling the phase-shift and the duty ratio of the bridges. The optimized duty cycle and phase shift are derived by optimization through Lagrange Multiplier and expressed in terms of measured supercapacitor and output voltages. The efficiency of the DAB operation with the proposed operating condition is measured to be above 90% at 20% voltage dip of the supercapacitor. Smoothing of oscillating power generated in a wave energy conversion system is presented as the test case of the application of the control system.

References

[1] P. T. Jacobson, G. Hagerman, and G. Scott, "Mapping and assessment of the United States ocean wave energy resource," Electric Power Research Institute, Tech. Rep., 2011.

[2] B. Czech and P. Bauer, "Wave energy converter concepts: design challenges and classification," *IEEE Ind. Electron. Mag.*, vol. 6, no. 2, pp. 4–16, Jun. 2012.

[3] L. Cameron, R. Doherty, A. Henry, K. Doherty, J. Vant Hoff, D. Kaye, D. Naylor, S. Bourdier, and T. Whittaker, "Design of the next generation of the oyster wave energy converter," in *Proc. IEEE Int. Conf. Ocean Energy (ICOE)*, vol. 6, Bilbao, Spain, Oct. 2010.

[4] S. Hazra and S. Bhattacharya, "An active filter-enabled power architecture for oscillating wave energy generation," *IEEE J. Emerg. Sel. Topics Power Electron.*, vol. 5, no. 2, pp. 723–734, Jun. 2017.

[5] M. Winter and R. J. Brodd, "What are batteries, fuel cells, and supercapacitors?" *Chemical reviews*, vol. 104, no. 10, pp. 4245–4270, 2004.

[6] S. Hazra and S. Bhattacharya, "Hybrid energy storage system comprising of battery and ultra-capacitor for smoothing of oscillating wave energy," in *Proc. IEEE Energy Convers. Congr. and Expo. (ECCE)*, Sep. 2016, pp. 1–8.

[7] M. Kheraluwala, R. W. Gascoigne, D. M. Divan, and E. D. Baumann, "Performance characterization of a high-power dual active bridge DC-to-DC converter," *IEEE Trans. Ind. Appl.*, vol. 28, no. 6, pp. 1294–1301, Nov.-Dec. 1992.

[8] A. K. Jain and R. Ayyanar, "PWM control of dual active bridge: Comprehensive analysis and experimental verification," *IEEE Transactions on Power Electronics*, vol. 26, no. 4, pp. 1215–1227, April 2011.

[9] C. Calderon, A. Barrado, A. Rodriguez, A. Lazaro, M. Sanz, and E. Olas, "Dual active bridge with triple phase shift, soft switching and minimum rms current for the whole operating range," in *IECON 2017 - 43rd Annual Conference of the IEEE Industrial Electronics Society*, 2017, pp. 4671–4676.

[10] A. Tong, L. Hang, G. Li, X. Jiang, and S. Gao, "Modeling and analysis of a dual-active-bridge-isolated bidirectional dc/dc converter to minimize rms current with whole operating range," *IEEE Transactions on Power Electronics*, vol. 33, no. 6, pp. 5302–5316, June 2018.

[11] W. Han, R. Ma, Q. Liu, and L. Corradini, "A conduction losses optimization strategy for dab converters in wide voltage range," in *IECON 2016 - 42nd Annual Conference of the IEEE Industrial Electronics Society*, Oct 2016, pp. 2445–2451.

[12] S. Hazra and S. Bhattacharya, "Modeling and emulation of a rotating paddle type wave energy converter," *IEEE Trans. Energy Convers.*, vol. PP, no. 99, pp. 1–1, 2017.